Soft Matter

PAPER

View Article Online
View Journal | View Issue

Cite this: *Soft Matter*, 2017, 13, 421

Equation of state for random sphere packings with arbitrary adhesion and friction

Wenwei Liu,[a] Yuliang Jin,[b] Sheng Chen,[a] Hernán A. Makse[c] and Shuiqing Li*[a]

Received 29th September 2016,
Accepted 29th November 2016

DOI: 10.1039/c6sm02216b

www.rsc.org/softmatter

We systematically generate a large set of random micro-particle packings over a wide range of adhesion and friction by means of adhesive contact dynamics simulation. The ensemble of generated packings covers a range of volume fractions ϕ from 0.135 ± 0.007 to 0.639 ± 0.004, and of coordination numbers Z from 2.11 ± 0.03 to 6.40 ± 0.06. We determine ϕ and Z at four limits (random close packing, random loose packing, adhesive close packing, and adhesive loose packing), and find a universal equation of state $\phi(Z)$ to describe packings with arbitrary adhesion and friction. From a mechanical equilibrium analysis, we determine the critical friction coefficient $\mu_{f,c}$: when the friction coefficient μ_f is below $\mu_{f,c}$, particles' rearrangements are dominated by sliding, otherwise they are dominated by rolling. Because of this reason, both $\phi(\mu_f)$ and $Z(\mu_f)$ change sharply across $\mu_{f,c}$. Finally, we generalize the Maxwell counting argument to micro-particle packings, and show that the loosest packing, *i.e.*, adhesive loose packing, satisfies the isostatic condition at Z = 2.

1 Introduction

Random packings of uniform spherical particles have been studied to model simple liquids, metallic and colloidal glasses, and granular materials.[1–3] In packings of large grains like glass beads, both elastic and frictional forces play important roles. In the frictionless case, the volume fraction ϕ is generally found around the random close packing (RCP) limit at $\phi_{RCP} \approx 0.64$.[1,2,4–6] The presence of friction substantially extends the volume fraction to a range $[\phi_{RLP}, \phi_{RCP}]$, where the lower limit $\phi_{RLP} \approx 0.55$ is often referred to as the random loose packing (RLP), corresponding to the large friction coefficient μ_f limit.[6–11] Furthermore, friction also has a significant impact on the isostatic condition of random packings. The minimal average coordination number, Z, required to obtain static packings is $Z = 4$ for $\mu_f = \infty$ and $Z = 6$ for $\mu_f = 0$.[12] While it is well known that RCP satisfies the isostatic condition, it has been reported that a frictional packing is also isostatic if one considers only interactions between asperities on contacting particles[13] or excludes fully mobilized contacts at the Coulomb threshold.[14,15]

For micro-particles, they are subject to not only elastic and frictional forces but also adhesive and electrostatic forces.[10,16,17] For instance, van der Waals forces become non-negligible and generally dominate interactions between micron-sized particles smaller than 10 μm. In this case, adhesive forces could distinctly change the structural and mechanical properties of packings.[16,18] However, despite the ubiquitous application of micro-particle packings in various areas such as engineering, biology, agriculture and physical sciences,[18–20] studies on such packings are limited.[17,20–24] In particular, little attention has been paid to the problem of how the adhesive packings change for arbitrary friction.

For micro-particle packings, simulations and experiments have found that both the volume fraction and the coordination number can go far below the RLP limit.[20–22,25] The lowest volume fraction reported in experiments is ϕ = 0.15 by random deposition of 1.5 μm particles in a vacuum.[20] Simulations suggest that there could exist a lower asymptotic limit, referred to as the adhesive loose packing (ALP) limit[24] at $\phi_{ALP} \approx 0.125$ and $Z_{ALP} \approx 2$, corresponding to infinitely adhesive and frictional packings. It has been shown that for a deposition process, the effect of electrostatic forces can be integrated into an effective adhesion, and thus the existence of electrostatic forces does not change the overall range of packing fractions.[17] The two major factors that determine the volume fraction and the coordination number are friction and adhesion. In this paper, we systematically study a large set of micro-particle packings over a wide range of adhesion and friction values. We confirm that ALP is indeed the lower limit of both ϕ and Z for the ensemble of our numerically generated packings. We also discover a new adhesive close packing (ACP) limit that corresponds to the case with zero adhesion and infinite friction.

[a] *Key Laboratory for Thermal Science and Power Engineering of Ministry of Education, Department of Thermal Engineering, Tsinghua University, Beijing 100084, China. E-mail: lishuiqing@tsinghua.edu.cn*
[b] *Cybermedia Center, Osaka University, Toyonaka, Osaka 560-0043, Japan*
[c] *Levich Institute and Physics Department, City College of New York, New York 10031, USA*

2 Discrete Element Method Simulation

We perform numerical simulations of micron-sized particles *via* the discrete element method (DEM).[16,18,26,27] The particles are soft, adhesive, frictional, and non-Brownian. The DEM framework used in this work is specifically developed for micro-particles.[16,18,28] Both the translational and rotational motions of each particle follow the Newton's second law,

$$m\frac{\mathrm{d}\boldsymbol{v}}{\mathrm{d}t} = \boldsymbol{F}_\mathrm{g} + \boldsymbol{F}_\mathrm{A},$$
$$I\frac{\mathrm{d}\Omega}{\mathrm{d}t} = \boldsymbol{M}_\mathrm{A}, \quad (1)$$

where $\boldsymbol{v}$ and $\boldsymbol{\Omega}$ are, respectively, the velocity and the rotation rate of an individual particle, m is the particle mass, and I is the moment of inertia. The system is assumed to be in a vacuum, so that fluid forces and torques are ignored. $\boldsymbol{F}_\mathrm{g}$ is the gravity. $\boldsymbol{F}_\mathrm{A}$ and $\boldsymbol{M}_\mathrm{A}$ denote the adhesive contact forces and the torques on the particle. They include

$$\mathbf{F}_\mathrm{A} = F_\mathrm{n}\boldsymbol{n} + F_\mathrm{s}\boldsymbol{t}_\mathrm{s},$$
$$\boldsymbol{M}_\mathrm{A} = r_\mathrm{p}F_\mathrm{s}(\boldsymbol{n}\times\boldsymbol{t}_\mathrm{s}) + M_\mathrm{r}(\boldsymbol{t}_\mathrm{s}\times\boldsymbol{n}) + M_\mathrm{t}\boldsymbol{n}, \quad (2)$$

where F_n is the normal force including the adhesively elastic contact force F_ne and the damping force F_nd, F_s is the tangential force due to the sliding friction, M_r is the rolling resistance and M_t is the twisting resistance. r_p is the particle radius. $\boldsymbol{n}$, $\boldsymbol{t}_\mathrm{s}$ and $\boldsymbol{t}_\mathrm{r}$ are the normal, tangential and rolling direction unit vectors, respectively.

A JKR (Johnson–Kendall–Roberts) model is applied to account for F_ne between the relatively compliant micro-particles.[29] The solid-phase dissipation force F_nd caused by the viscoelasticity of materials is assumed to be proportional to the rate of change of material deformation. Thus, the normal force F_n is given by

$$F_\mathrm{n} = F_\mathrm{ne} + F_\mathrm{nd} = 4F_\mathrm{C}\left[\left(\frac{a}{a_0}\right)^3 - \left(\frac{a}{a_0}\right)^{3/2}\right] + \eta_\mathrm{N}\upsilon_\mathrm{R}\cdot\boldsymbol{n}, \quad (3)$$

where F_C is the critical pull-off force expressed by the surface energy γ: $F_\mathrm{C} = 3\pi\gamma R$, a is the radius of the contact area with a_0 at equilibrium in the JKR model, η_N is the normal dissipation coefficient and $\boldsymbol{v}_\mathrm{R}$ is the relative velocity at the contact point on particle surfaces. Here R is defined as the effective radius between two contacting particles, $1/R = 1/r_{\mathrm{p}_1} + 1/r_{\mathrm{p}_2}$.

The dissipative friction terms, including the sliding, twisting and rolling terms in the presence of adhesion, are all approximated by a spring–dashpot–slider model with model parameters given in ref. 16 and 30. The slider considerations mean that the sliding, twisting and rolling resistances all reach critical values, $F_\mathrm{s,crit}$, $M_\mathrm{t,crit}$ and $M_\mathrm{r,crit}$, when corresponding displacements exceed certain limits. Once these limits are reached, the particles start to slide or spin, and the resistances remain unchanged at the critical values, which are given by

$$F_\mathrm{s,crit} = \mu_\mathrm{f}|F_\mathrm{ne} + 2F_\mathrm{C}|,$$

$$M_\mathrm{t,crit} = 3\pi a F_\mathrm{s,crit}/16,$$

$$M_\mathrm{r,crit} = -4F_\mathrm{C}(a/a_0)^{3/2}\Theta_\mathrm{crit}R. \quad (4)$$

Here Θ_crit is the critical angle for the relative rolling between two particles. The values or ranges of Θ_crit and γ are selected according to the data obtained from atomic force microscopy measurements.[31,32] The long-range electrostatic interactions are neglected because their effects on ϕ and Z can be integrated into an effective adhesion parameter.[17]

As shown in Fig. 1, our simulation starts from the sequential adding of 1000 spheres of radius r_p from an inlet plane at a height H with an initial velocity U_0 under gravity. The initial position of each particle at the inlet is randomly decided. The direction of U_0 is the same as that of gravity, pointing to the positive of the x-axis. The gravitational effect on the deposition process is negligible due to the small time duration. This distinguishes our system from those in ref. 21 and 25, which generate particles randomly in a box without touching each other and allow them to deposit under gravity. Periodic boundary conditions are set along the two horizontal directions of length L. The physical parameters used in the simulations, including the particle size, the surface energy, *etc.*, are all listed in Table 1. The friction coefficient is changed from $\mu_\mathrm{f} = 10^{-5}$ to $\mu_\mathrm{f} = 10$. It can be shown that for this setup, the volume fraction and the coordination number only depend on two independent parameters, the friction coefficient μ_f and the dimensionless adhesion parameter,[17,24]

$$\mathrm{Ad} = \gamma/(\rho_\mathrm{p}U_0{}^2R), \quad (5)$$

where ρ_p is the mass density. The adhesion parameter Ad combines the effects of particle velocity, size and adhesion.

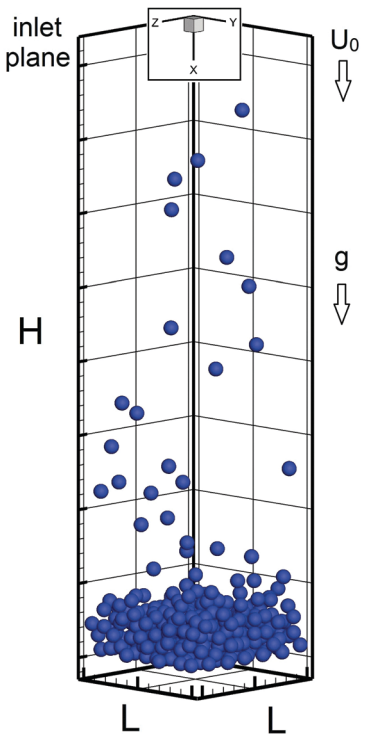

Fig. 1 A schematic of the simulation domain.

Table 1 Parameters used in DEM simulations of micro-particle packings

Parameter	Value	Unit
Simulation box length (L)	$20r_p$	μm
Falling height (H)	$4L$	μm
Particle radius (r_p)	1, 5, 10, 50	μm
Mass density (ρ_p)	2500	kg m^{-3}
Surface energy (γ)	0.05–15	mJ m^{-2}
Initial velocity (U_0)	0.5	m s^{-1}
Friction coefficient (μ_f)	10^{-5}–10	

Fig. 2 shows the dependence of the volume fraction ϕ and the coordination number Z on the friction coefficient μ_f, for several fixed adhesion parameters Ad. For each fixed Ad, both ϕ and Z reach their upper limits when $\mu_f \leq 10^{-4}$, and decrease with the increase of μ_f until their lower limits are obtained when $\mu_f > 1$ (Fig. 2(a) and (b)). Fitting the data to constants for $\mu_f \leq 10^{-4}$ ($\mu_f > 1$) gives the maximum (minimum) values of ϕ and Z for each Ad. The maximum $Z_{max} \approx 6$ is independent of Ad, which corresponds to the isostatic condition of frictionless sphere packings. This result indicates that adhesion has no effect on the coordination number when friction is sufficiently small. The other asymptotic values ϕ_{max}, ϕ_{min} and Z_{min} are all Ad-dependent, and can be fitted to exponential laws (Fig. 2(c) and (d)),

$$\phi_{max}(\mathrm{Ad}) = \phi_{RLP} + a_1 e^{-\lambda_1 \mathrm{Ad}}$$
$$\phi_{max}(\mathrm{Ad}) = \phi_{ALP} + a_2 e^{-\lambda_2 \mathrm{Ad}}$$
$$Z_{min}(\mathrm{Ad}) = Z_{ALP} + b e^{-\xi \mathrm{Ad}} \quad (6)$$

where $a_1 = 0.145$, $\lambda_1 = 0.159$, $a_2 = 0.415$, $\lambda_2 = 0.123$, $b = 1.74$, and $\xi = 0.13$. As discussed in ref. 24, Ad = 1 is a critical threshold below which the adhesion is negligible. Thus, in this paper, we define Ad = 1 as the adhesionless limit. Note that in ref. 24, only one fixed value $\mu_f = 0.3$ is used, which lies in the asymptotic regime $\mu_f > 0.1$.

Based on the above results (Fig. 2 and eqn (6)), we extrapolate four limits for the ensemble of micro-particle packings

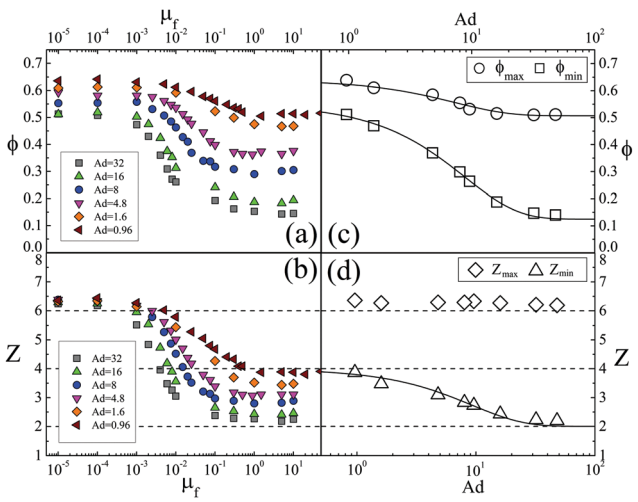

Fig. 2 (a) The volume fraction ϕ and (b) the coordination number Z of random micro-particle packings are plotted as functions of μ_f, for a few fixed Ad. The asymptotic values (c) ϕ_{min}, ϕ_{max}, (d) Z_{max} and Z_{min} are plotted as a function of Ad. The solid lines are exponential fittings according to eqn (6). The dashed lines are Z^{iso} derived from isostatic conditions (Table 2).

Table 2 Volume fraction ϕ and coordination number Z at four limits of random micro-particle packings. The Z^{iso} values are isostatic values obtained from the counting argument

	Ad	μ_f	ϕ	Z	Z^{iso}
RCP	1	0	0.639 ± 0.004	6.4 ± 0.06	6
RLP	1	∞	0.512 ± 0.004	3.87 ± 0.04	4
ACP	∞	0	0.512 ± 0.002	6.19 ± 0.04	6
ALP	∞	∞	0.135 ± 0.007	2.11 ± 0.02	2

generated by our numerical protocol: the random close packing RCP, the random loose packing RLP, the adhesive close packing ACP, and the adhesive loose packing ALP (see Table 2). At RCP and RLP, our volume fractions $\phi_{RCP} = 0.639$ and $\phi_{RLP} = 0.512$ are close to the previously reported values $\phi_{RCP} \approx 0.64$[1,4,6] and $\phi_{RLP} \approx 0.55$.[6–11] The coordination numbers $Z_{RCP} = 6.4$ and $Z_{RLP} = 3.87$ are close to the isostatic condition $Z_{RCP} = 6$ and $Z_{RLP} = 4$. A little higher Z_{RCP} is due to the compression caused by particle inertia. The values $\phi_{ALP} = 0.135$ and $Z_{ALP} = 2.11$ are close to the conjecture $\phi_{ALP} = 0.125$ and $Z_{ALP} = 2$.[24] As for ACP, similar results of $\phi_{ACP} = 0.569$ and $Z_{ACP} = 6.09$ has been found in DEM simulations with $\mu_f = 0.2$.[23] We point out that these limits are obtained within our protocol, and their values might change in another protocol.[2,5] The well-defined lower bound at $\phi_{ALP} = 0.135$ is in contrast to ref. 10, which argues that there is no lowest volume fraction for cohesive and frictional packings.

3 Equation of state

Next we show that the volume fraction ϕ and the coordination number Z of micro-particle packings follow a simple universal equation of state (EOS),

$$\frac{1}{\phi} - 1 = \frac{C}{Z^\gamma}, \quad (7)$$

where both parameters C and γ depend on Ad (see Fig. 3). In the adhesionless limit, $C(\mathrm{Ad} \to 1) \to 2\sqrt{3}$ and $\gamma(\mathrm{Ad} \to 1) \to 1$, which are consistent with the theoretical EOS of adhesionless packings $\phi = Z/(Z + 2\sqrt{3})$.[6] The left-hand side term $\frac{1}{\phi} - 1$ in eqn (7) is equal to reduced free volume function ω, which is defined as $\omega = (W - V_g)/W$, where W is the average volume of the Voronoi cell of each particle, and V_g is the volume of a particle. Eqn (7) suggests a simple power-law relation between ω and Z (see Fig. 3(b)),

$$\omega = \frac{C}{Z^\gamma}. \quad (8)$$

The EOSs, eqn (7) and (8) work well for most of the simulation data; exceptions are found when $\mu_f > 0.1$ for the largest Ad = 48, where small deviations from eqn (7) and (8) are observed.

The power-law scaling of the macroscopic EOS, eqn (8), implies an invariant property of a probability distribution function (PDF) that describes Voronoi cell boundaries. It can be shown that ω is related to the PDF $p(\omega^s)$ of the orientational reduced free volume function ω^s (see Fig. 4(a)),

$$\omega = \int_0^\infty \omega^s p(\omega^s) \mathrm{d}\omega^s, \quad (9)$$

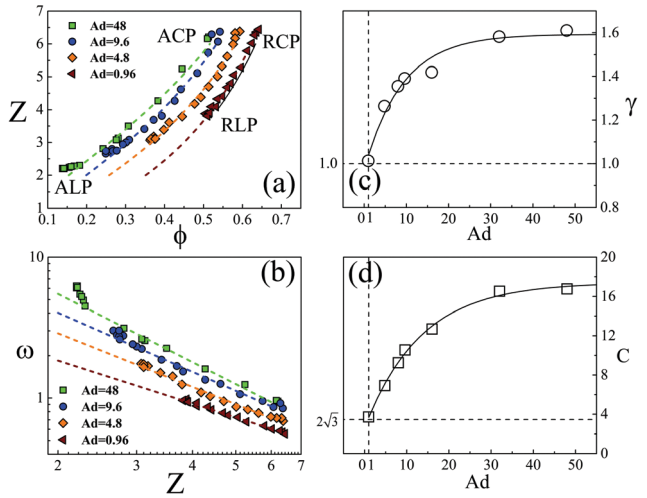

Fig. 3 (a) Simulation data $\phi(Z)$ (points) of micro-particle packings with a few different Ad values, where for each fixed Ad, the friction coefficient μ_f is varied from 10^{-5} to 10 (see Fig. 2). The solid line is the theoretical prediction for non-adhesive packings in ref. 6. The dotted lines are fittings to the EOS, eqn (7). (b) Simulation data $\omega(Z)$ (points) are compared to the EOS, eqn (8) (dotted lines), on log–log scales. The fitting parameters γ and C are given in (c) and (d), respectively.

where $\omega^s = (\ell/r_p)^3 - 1$ and ℓ is the distance from the center of a particle to its Voronoi boundary (VB). Both $p(\omega^s)$ and its inverse cumulative distribution function (ICDF) $P_>(\omega^s) = 1 - \int_0^{\omega^s} p(x)\mathrm{d}x$ depend on μ_f and Ad. Eqn (8) and (9) suggest that $P_>(\omega^s)$ should have a form (the dependence on μ_f and Ad are shown explicitly)

$$P_>(\omega^s;\mu_f,\mathrm{Ad}) = q(\mathrm{Ad})F[\omega^s Z(\mu_f,\mathrm{Ad})^{\gamma(\mathrm{Ad})};\mathrm{Ad}], \qquad (10)$$

where the prefactor q and the functional form of $F(x)$ only depend on Ad but not μ_f. Indeed, substituting eqn (10) in eqn (9) recovers the EOS, eqn (8). Eqn (10) shows that for any fixed Ad, if one plots $P_>(\omega^s)$ (or $p(\omega^s)$) as a function of $\omega^s Z^\gamma$, the data at different μ_f values should collapse onto a master curve, which is confirmed in Fig. 4. Note that $P_>(\omega^s)$ is essentially related to n-particle correlation functions g_n for all orders of n.[33] Thus the collapse of $P_>(\omega^s)$ reveals some invariant property of correlations between particles under different frictions. This invariant property is not incorporated into the standard pair correlation function $g_2(r)$, since its corresponding ICDF $P_>(\omega^r)$ does not collapse on a rescaled plot as a function of $\omega^r Z^\gamma$, where $\omega^r = (r/2r_p)^3 - 1$ is the free-volume-like parameter associated with the inter-particle distance r (see Fig. 4).

4 Mechanical equilibrium analysis

In micro-particle packings, the coordination number Z can reach as low as two, which is way below the isostatic condition $Z = 6$ for non-adhesive frictionless packings. Indeed, in our simulations, a large number of particles with only one or two contacts can be mechanically stabilized. For the simplest case shown in Fig. 5, we explain how adhesion and friction make particles with one contact (the top particle p_1 in the inset of Fig. 5) reach mechanical equilibrium. Without adhesion, the particle p_1 would never be stabilized except for $\theta = 0^\circ$. However, in the presence of adhesion, when two contact particles start to or have the tendency to roll, the rear side of the contact surface will remain in touch instead of detaching immediately, until the critical pull-off force F_C is reached. This process is known as the necking process. As a consequence, the attractive normal stress on the rear side will provide additional rolling resistance to prevent the particle from rolling over. The competition between the rolling (pull-off condition) and sliding (Coulomb friction law) conditions determines the stability condition for the particle (see Appendix). Fig. 5 shows the mechanical equilibrium diagram in terms of angle θ and the normalized external force F_{ext}/F_C, for particles with $Z = 1$. The area under

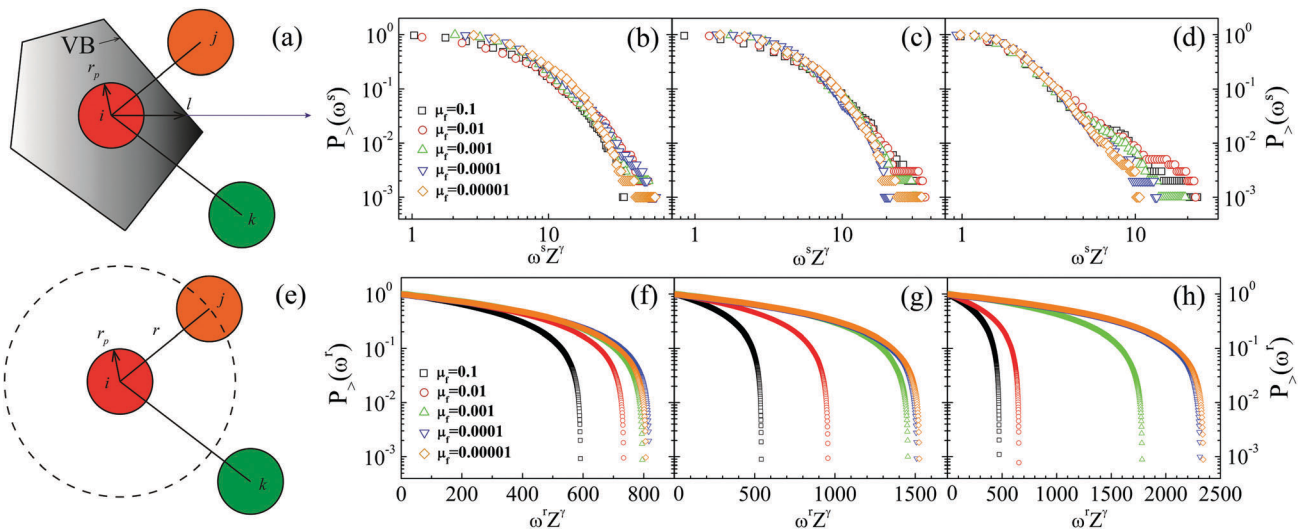

Fig. 4 (a) Two-dimensional illustration of the definition of ℓ. The inverse cumulative distribution functions $P_>(\omega^s)$ at different μ_f values are plotted as a function of $\omega^s Z^\gamma$, for (b) Ad = 48, (c) Ad = 8 and (d) Ad = 0.96, respectively. (e) Two-dimensional illustration of the definition of r. The inverse cumulative distribution functions $P_>(\omega^r)$ at different μ_f values are plotted as a function of $\omega^r Z^\gamma$, for (f) Ad = 48, (g) Ad = 8 and (h) Ad = 0.96, respectively.

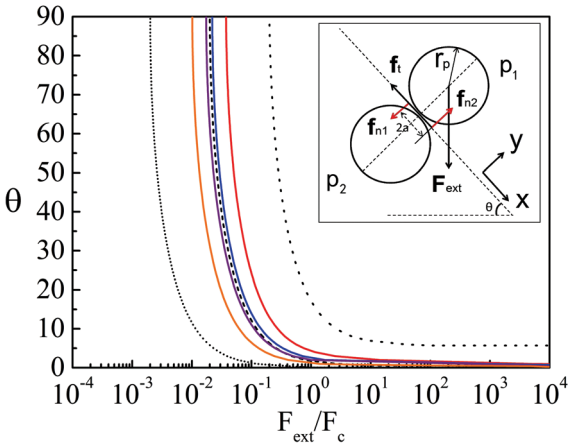

Fig. 5 Mechanical equilibrium diagram of micro-particles with one contact. The solid lines are rolling equilibrium lines for r_p = 1, 5, 10, 50 μm (from right to left). The others are sliding equilibrium lines with μ_f = 0.1, 0.01, and 0.001 (from right to left). The area under the lines indicates the equilibrium region that the particle does not roll or slide. The inset shows the schematic of force and torque balance conditions.

the lines indicates the equilibrium region of the corresponding friction condition. We can see that for each fixed μ_f, the particle can even be stabilized at $\theta = 90^\circ$, as long as the external force F_{ext} is sufficiently small, which would never happen in non-adhesive packings. When $\mu_f > \mu_{f,c}$, where $\mu_{f,c}$ is a critical friction coefficient (for instance $\mu_{f,c} \approx 0.01$ for r_p = 5 μm as indicated in Fig. 5), the rolling equilibrium line lies under the sliding equilibrium line, implying that particles roll first before they begin to slide. In this case, the rearrangement during the packing formation is dominated by rolling, which agrees well with the fact that rolling is generally the preferred deformation mode for small adhesive particles.[18,19] On the other hand, when $\mu_f < \mu_{f,c}$, sliding lines shift to the left of the rolling line. In this case, the additional rolling resistance caused by adhesion is not able to hold the particle and it will slide first, leading to a prominent rearrangement of its position. Although here we only consider the simplest case Z = 1, Fig. 2 shows that both $\phi(\mu_f)$ and $Z(\mu_f)$ indeed have a steep change around $\mu_f \sim \mu_{f,c}$, indicating the separation of rolling- and sliding-dominant regimes.

5 Isostatic condition

To further understand the behavior of coordination number Z as shown in Fig. 2(b), we generalize the Maxwell counting argument for the isostatic condition.[6,34] A packing is isostatic when the degree of freedom equals the number of constraints:

$$N_n + N_t + N_T = E_f + E_t, \quad (11)$$

where N_n, N_t, N_T, E_f, and E_t are the total numbers of normal forces, tangential forces, additional contacting torques caused by adhesion, force balance equations, and torque balance equations, respectively. It should be noted that in the Maxwell counting argument for non-adhesive cases, the real forces are assumed to be point forces acting at the exact contact point, *i.e.* the center of the contact surface, since they are symmetrically distributed in the contact surface. As a result, all the torques in the torque balance equations originate from the point forces and there are no undetermined torque variables. However, for adhesive micron-sized particles, the phenomenon of material "necking" gives rise to an asymmetry of the forces in the contact region, leading to the additional torque variable N_T.

Table 3 Number of constraints and degrees of freedom determining the isostatic condition in micro-particle packings

Parameters	N_n	N_t	N_T	E_f	E_t	Z^{iso}
$\mu_f = 0$, any Ad	$\frac{1}{2}NZ$	0	0	$3N$	0	6
$\mu_f = \infty$, Ad = 1	$\frac{1}{2}NZ$	NZ	0	$3N$	$3N$	4
$\mu_f = \infty$, Ad = ∞	$\frac{1}{2}NZ$	NZ	$\frac{3}{2}NZ$	$3N$	$3N$	2

From the analysis of the isostatic condition eqn (11), we obtain the coordination number for three special cases (see Table 3). (i) In frictionless packings (μ_f = 0), each contact has one normal force $\left(N_n = \frac{1}{2}NZ\right)$ and no tangential forces (N_t = 0). The contact forces are distributed symmetrically in the contact area regardless of whether there is adhesion or not and therefore do not generate torques (N_T = 0). In this case, the isostatic condition gives $Z^{iso}(\mu_f = 0, \text{Ad}) = Z^{iso}_{RCP} = Z^{iso}_{ACP} = 6$. (ii) In infinitely frictional and non-adhesive packings ($\mu_f = \infty$, Ad = 1, RLP limit),[6] each contact has two additional tangential forces in orthogonal directions ($N_t = NZ$). In addition to three independent force balance equations ($E_f = 3N$), each particle also needs to satisfy three independent torque balance equations (E_t = 3N). Solving eqn (11) gives $Z^{iso}_{RLP} = 4$. (iii) In infinitely frictional and infinitely adhesive packings ($\mu_f = \infty$, Ad = ∞, ALP limit), each contact provides three additional independent torque variables $\left(N_T = \frac{3}{2}NZ\right)$, which result from the asymmetry of the contact forces. In this case, eqn (11) predicts $Z^{iso}_{ALP} = 2$. We do not discuss the general case with arbitrary μ_f and Ad, for which first-principles analysis is unavailable.

6 Conclusions

In summary, the influence of friction on random adhesive loose packings of uniform spherical micro-particles is examined by using adhesive DEM simulations. The volume fraction and the coordination number can be well characterized by two dimensionless parameters μ_f and Ad, and are found to follow a universal equation of state $\phi(Z)$. Our results significantly extend the existing phase diagram of random packings.[6,24]

For the ensemble of packings generated in our simulations, we find a new ACP limit that is corresponding to Ad = ∞ and μ_f = 0. We also confirm the ALP limit reported in previous studies.[17,24] It would be interesting to examine these limits in experiments. The lowest reported experimental packing fraction is ϕ = 0.15,[20] which is above but not too far away from our ϕ_{ALP} = 0.135 ± 0.007. Our numerical protocol – depositing micro-particles randomly into a vacuum container – basically resembles the experiments in ref. 20. Our results suggest that

the loosest packing generated in such procedures shall be sought under maximum friction and adhesion.

Appendix A: derivation of the mechanical equilibrium diagram

The inset in Fig. 5 shows the force traction of two contact particles in two dimensions. We consider the mechanical equilibrium of the top particle p_1. Two force equations and one torque equation must be satisfied to make p_1 reach mechanical equilibrium, which can be written as

$$\begin{aligned} F_{\text{ext}}\sin\theta - f_{\text{t}} &= 0, \\ -F_{\text{ext}}\cos\theta - f_{\text{n1}} + f_{\text{n2}} &= 0, \\ F_{\text{ext}} r_{\text{p}}\sin\theta - \tfrac{1}{2}a(f_{\text{n1}} + f_{\text{n2}}) &= 0 \end{aligned} \tag{A1}$$

Here the normal stress is simplified into two point forces f_{n1} and f_{n2}. It should be noted that for adhesive micron-sized particles, f_{n1} is usually attractive due to the material "necking", while for non-adhesive granular matter, both f_{n1} and f_{n2} are repulsive. Solving eqn (A1), we obtain

$$\begin{aligned} f_{\text{t}} &= F_{\text{ext}}\sin\theta, \\ f_{\text{n1}} &= \frac{F_{\text{ext}}}{2}\left(\frac{2r_{\text{p}}\sin\theta}{a} - \cos\theta\right), \\ f_{\text{n2}} &= \frac{F_{\text{ext}}}{2}\left(\frac{2r_{\text{p}}\sin\theta}{a} + \cos\theta\right). \end{aligned} \tag{A2}$$

To keep particle p_1 mechanically balanced, the Coulomb friction law in the presence of adhesion must be satisfied, as shown in eqn (4). We also must make sure that the pull-off does not occur, which means that $f_{\text{n1}} \le \frac{1}{2}F_{\text{C}}$. Therefore, the conditions to guarantee the balance of particle p_1 are then

$$\begin{aligned} f_{\text{t}} &\le \mu_{\text{f}}\left(-f_{\text{n1}} + f_{\text{n2}} + 2F_{\text{C}}\right), \\ f_{\text{n1}} &\le \tfrac{1}{2}F_{\text{C}} \end{aligned} \tag{A3}$$

Substituting eqn (A2) into inequation (A3), we have

$$\begin{aligned} \frac{F_{\text{ext}}}{F_{\text{C}}} &\le \frac{2\mu_{\text{f}}}{\sin\theta - \mu_{\text{f}}\cos\theta}, \\ \frac{F_{\text{ext}}}{F_{\text{C}}} &\le \frac{1}{\dfrac{2r_{\text{p}}\sin\theta}{a} - \cos\theta}. \end{aligned} \tag{A4}$$

Here the equilibrium radius of the contact surface in the JKR model $a_0 = \left(\dfrac{9\pi\gamma R^2}{2E}\right)^{1/3}$ is applied to estimate a, where E represents the elasticity of particles. By changing μ_{f} and θ in inequation (A4), we can draw the mechanical equilibrium diagram.

Acknowledgements

This work has been funded by the National Natural Science Funds of China (No. 51390491) and the National Key Basic Research Program of China (No. 2013CB228506). H. A. Makse acknowledges funding from NSF and DOE. We thank Profs. M. Doi, N. V. Brilliantov, and J. S. Marshall for fruitful discussions on the contact dynamic model, and Dr G. Liu, M. Yang, H. Zhang, Mr R. Tao, and W. Shi for their useful suggestions.

References

1 J. D. Bernal, *Nature*, 1959, **183**, 141–147.
2 G. Parisi and F. Zamponi, *Rev. Mod. Phys.*, 2010, **82**, 789–845.
3 A. Coniglio, A. Fierro, H. J. Herrmann and M. Nicodemi, *Unifying Concepts in Granular Media and Glasses: From the Statistical Mechanics of Granular Media to the Theory of Jamming*, Elsevier, 2004.
4 C. S. O'Hern, L. E. Silbert, A. J. Liu and S. R. Nagel, *Phys. Rev. E: Stat., Nonlinear, Soft Matter Phys.*, 2003, **68**, 011306.
5 S. Torquato and F. H. Stillinger, *Rev. Mod. Phys.*, 2010, **82**, 2633–2672.
6 C. Song, P. Wang and H. A. Makse, *Nature*, 2008, **453**, 629–632.
7 G. Y. Onoda and E. G. Liniger, *Phys. Rev. Lett.*, 1990, **64**, 2727–2730.
8 M. P. Ciamarra and A. Coniglio, *Phys. Rev. Lett.*, 2008, **101**, 128001.
9 M. Jerkins, M. Schröter, H. L. Swinney, T. J. Senden, M. Saadatfar and T. Aste, *Phys. Rev. Lett.*, 2008, **101**, 018301.
10 K. J. Dong, R. Y. Yang, R. P. Zou and A. B. Yu, *Phys. Rev. Lett.*, 2006, **96**, 145505.
11 G. R. Farrell, K. M. Martini and N. Menon, *Soft Matter*, 2010, **6**, 2925–2930.
12 L. E. Silbert, D. Ertas, G. S. Grest, T. C. Halsey and D. Levine, *Phys. Rev. E: Stat., Nonlinear, Soft Matter Phys.*, 2002, **65**, 031304.
13 S. Papanikolaou, C. S. O'Hern and M. D. Shattuck, *Phys. Rev. Lett.*, 2013, **110**, 198002.
14 K. Shundyak, M. van Hecke and W. van Saarloos, *Phys. Rev. E: Stat., Nonlinear, Soft Matter Phys.*, 2007, **75**, 010301.
15 S. Henkes, M. van Hecke and W. van Saarloos, *Europhys. Lett.*, 2010, **90**, 14003.
16 S. Li, J. S. Marshall, G. Liu and Q. Yao, *Prog. Energy Combust. Sci.*, 2011, **37**, 633–668.
17 S. Chen, S. Li, W. Liu and H. A. Makse, *Soft Matter*, 2016, **12**, 1836–1846.
18 J. S. Marshall and S. Li, *Adhesive Particle Flow*, Cambridge University Press, 2014.
19 C. Dominik and A. G. G. M. Tielens, *Astrophys. J.*, 1997, **480**, 647.
20 J. Blum and R. Schräpler, *Phys. Rev. Lett.*, 2004, **93**, 115503.
21 E. J. R. Parteli, J. Schmidt, C. Blumel, K.-E. Wirth, W. Peukert and T. Poschel, *Sci. Rep.*, 2014, **4**, 06227.
22 J. M. Valverde, M. A. S. Quintanilla and A. Castellanos, *Phys. Rev. Lett.*, 2004, **92**, 258303.
23 C. L. Martin and R. K. Bordia, *Phys. Rev. E: Stat., Nonlinear, Soft Matter Phys.*, 2008, **77**, 031307.
24 W. Liu, S. Li, A. Baule and H. A. Makse, *Soft Matter*, 2015, **11**, 6492–6498.
25 R. Y. Yang, R. P. Zou and A. B. Yu, *Phys. Rev. E: Stat. Phys., Plasmas, Fluids, Relat. Interdiscip. Top.*, 2000, **62**, 3900–3908.

26 N. V. Brilliantov, F. Spahn, J.-M. Hertzsch and T. Pöschel, *Phys. Rev. E: Stat. Phys., Plasmas, Fluids, Relat. Interdiscip. Top.*, 1996, **53**, 5382–5392.
27 N. V. Brilliantov, N. Albers, F. Spahn and T. Pöschel, *Phys. Rev. E: Stat., Nonlinear, Soft Matter Phys.*, 2007, **76**, 051302.
28 J. Marshall, *J. Comput. Phys.*, 2009, **228**, 1541–1561.
29 K. L. Johnson, K. Kendall and A. D. Roberts, *Proc. R. Soc. London, Ser. A*, 1971, **324**, 301–313.
30 M. Yang, S. Li and Q. Yao, *Powder Technol.*, 2013, **248**, 44–53.
31 L.-O. Heim, J. Blum, M. Preuss and H.-J. Butt, *Phys. Rev. Lett.*, 1999, **83**, 3328–3331.
32 B. Sümer and M. Sitti, *J. Adhes. Sci. Technol.*, 2008, **22**, 481–506.
33 Y. Jin and H. A. Makse, *Physica A*, 2010, **389**, 5362–5379.
34 S. Alexander, *Phys. Rep.*, 1998, **296**, 65–236.